

# Hybrid Precoding for mmWave Massive MIMO with One-Bit DAC

Sung Joon Maeng, Yavuz Yapıcı, İsmail Güvenç, Huaiyu Dai, and Arupjyoti Bhuyan

**Abstract**—Hybrid beamforming is key to achieving energy-efficient 5G wireless networks equipped with massive amount of antennas. Low-resolution data converters bring yet another degree of freedom to energy efficiency for the state-of-the-art 5G transceivers. In this work, we consider the design of hybrid precoders for massive multiple-input multiple-output (MIMO) channels in millimeter-wave (mmWave) spectrum along with one-bit digital-to-analog converters (DACs) and finite-quantized phase shifters. In particular, we propose an alternating-optimization-based precoder design which recursively computes the covariance of the quantization distortion, and updates the precoders accordingly. Numerical results verify that the achievable rate improves quickly through iterations that involve updates to the weight matrix, distortion covariance of the quantization, and the respective precoders.

**Index Terms**—5G, hybrid precoding, massive MIMO, mmWave communications, one-bit DAC.

## I. INTRODUCTION

The vastly unoccupied mmWave frequency band has been envisioned as a promising solution to spectrum scarcity over the conventional sub-6GHz communications [1]. The high path loss in mmWave frequencies should be compensated by effective beamforming strategies. Thanks to the form factors getting smaller in mmWave spectrum, it becomes possible to squeeze large antenna arrays even in mobile devices, and obtain sufficiently large beamforming gains. The energy efficiency, however, emerges as a concern when employing large antenna arrays, since conventional implementation (i.e., full-digital) requires a dedicated data converter (i.e., analog-to-digital converter (ADC), DAC) and radio-frequency (RF) chain (e.g., mixer, oscillator) for each antenna element. The hybrid beamforming, on the other hand, splits the overall precoding into the baseband and RF stages, which in turn cuts down the required number of data converters and RF chains, and, hence, improves energy efficiency [2].

The data converters with large bandwidth than ever before, which are particularly critical in mmWave communications, require exponentially increasing power consumption for integer number of resolution bits [3]. At the transmitter side with relatively larger antenna arrays, it is even more challenging to achieve desired beamforming gains at moderate power budgets. In this work, we therefore consider the hybrid precoder design for mmWave transmitters assuming one-bit DAC and massive MIMO.

There are limited number of works in the literature considering hybrid precoding along with low-resolution data converters, which generally assume low-resolution data converters at the receiver side (i.e., few-bit ADCs, infinite-resolution DACs). In particular, [4] considers two different hybrid precoder designs, which are based on channel inversion and

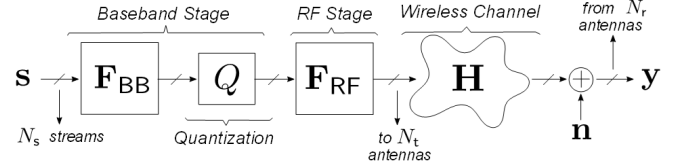


Fig. 1. System model for the point-to-point mmWave MIMO downlink with hybrid precoding and one-bit DAC.

singular value decomposition (SVD), for mmWave channels with few-bit ADCs. A hybrid precoder is proposed in [5] for point-to-point MIMO downlink assuming spatially uncorrelated channel and one-bit ADCs. In a recent study of [6], a hybrid precoder design based solely on SVD is proposed for spatially uncorrelated MIMO channels with few-bit DACs.

In this work, we propose a novel hybrid precoder for spatially correlated mmWave channels with one-bit DAC and finite-quantized phase shifters. In particular, contribution of the quantization distortion is carefully taken into account through recursive computation of the respective covariance matrix (instead of assuming a zero covariance [6]), which produces more reliable achievable rates. As a complete precoder design, we develop a novel alternating-maximization strategy where the baseband and RF precoders are updated iteratively relying on the Bussgang theorem [7], which is superior to additive quantization noise model (AQNM) [8] adopted by [4]–[6]. The numerical results verify the effectiveness of the proposed precoder design.

## II. SYSTEM MODEL

We consider a point-to-point massive MIMO downlink in mmWave spectrum, as illustrated in Fig. 1, where a transmitter equipped with  $N_t$  antennas and  $N_{RF}$  RF chains sends  $N_s$  data streams to a receiver with  $N_r$  antennas. Considering  $N_t$  being typically large, we assume a hybrid precoder at the transmitter with one-bit DACs to relieve the complexity and improve the energy efficiency, and infinite-resolution ADCs at the receiver, thanks to relatively smaller  $N_r$ .

Assuming  $\mathbf{F}_{RF} \in \mathbb{C}^{N_t \times N_{RF}}$ ,  $\mathbf{F}_{BB} \in \mathbb{C}^{N_{RF} \times N_s}$ , and  $\mathbf{s} \in \mathbb{C}^{N_s \times 1}$  are the analog RF precoder, digital baseband precoder, and transmitted data, respectively, the received signal is

$$\mathbf{y} = \mathbf{H}\mathbf{F}_{RF}\mathbf{Q}(\mathbf{F}_{BB}\mathbf{s}) + \mathbf{n}, \quad (1)$$

where  $\mathbf{Q}(\cdot)$  is one-bit quantization, and  $\mathbf{n}$  is the observation noise composed of independent complex Gaussian entries with zero-mean and variance  $\sigma_n^2$ . We also assume that  $\mathbb{E}[\mathbf{s}\mathbf{s}^H] = \frac{P_s}{N_s}\mathbf{I}_{N_s}$  where  $P_s$  is the total power of the unprecoded data, and  $\mathbf{I}_{N_s} \in \mathbb{R}^{N_s \times N_s}$  is the identity matrix. In (1),  $\mathbf{H} \in \mathbb{C}^{N_r \times N_t}$  represents the spatially correlated mmWave channel with  $N_c$  clusters and  $N_p$  rays [1].

### III. LINEAR QUANTIZATION MODELS

We consider two linearization schemes for the non-linear quantization operator  $\mathcal{Q}(\cdot)$  while deriving the desired precoders. The first scheme is AQNM [8], which is widely adopted—thanks to its simplicity—although it is known to overestimate the achievable rate performance especially for the small number of quantization bits [4], [9]. The respective linearization is expressed as follows

$$\mathcal{Q}(\mathbf{F}_{\text{BB}}\mathbf{s}) \approx \mathbf{A}_{\text{Q}}\mathbf{F}_{\text{BB}}\mathbf{s} + \mathbf{q}_{\text{Q}}, \quad (2)$$

where  $\mathbf{A}_{\text{Q}}$  is the weight matrix given as

$$\mathbf{A}_{\text{Q}} = \sqrt{1 - \eta_b} \mathbf{I}_{N_s}, \quad (3)$$

with  $\eta_b$  being the distortion factor, which is generally approximated by  $\eta_b \approx \frac{\pi\sqrt{3}}{2} 2^{-2b}$  for  $b$ -bit quantization with sufficiently large  $b$ , while its more accurate value for one-bit quantization is  $\eta_b \approx 0.3634$  [10]. In (2),  $\mathbf{q}_{\text{Q}}$  stands for the quantization distortion with the covariance

$$\mathbf{C}_{\mathbf{q}_{\text{Q}}\mathbf{q}_{\text{Q}}} = \mathbb{E}[\mathbf{q}_{\text{Q}}\mathbf{q}_{\text{Q}}^H] = \frac{P_s}{N_s} \eta_b (1 - \eta_b) \text{diag}(\mathbf{F}_{\text{BB}}\mathbf{F}_{\text{BB}}^H), \quad (4)$$

which seemingly ignores the correlation between the entries of  $\mathbf{q}_{\text{Q}}$  (i.e.,  $\mathbf{C}_{\mathbf{q}_{\text{Q}}\mathbf{q}_{\text{Q}}}$  is diagonal) that is the basic reason behind its not-sufficiently-accurate rates.

The second model we consider is based on the Bussgang theorem [7], which suggest the following decomposition

$$\mathcal{Q}(\mathbf{F}_{\text{BB}}\mathbf{s}) \approx \mathbf{A}_{\text{B}}\mathbf{F}_{\text{BB}}\mathbf{s} + \mathbf{q}_{\text{B}}, \quad (5)$$

where  $\mathbf{A}_{\text{B}}$  is the weight matrix given as

$$\mathbf{A}_{\text{B}} = \sqrt{\frac{2}{\pi}} [\text{diag}(\mathbf{C}_{\text{xx}})]^{-\frac{1}{2}} = \sqrt{\frac{2N_s}{\pi P_s}} [\text{diag}(\mathbf{F}_{\text{BB}}\mathbf{F}_{\text{BB}}^H)]^{-\frac{1}{2}}, \quad (6)$$

with  $\mathbf{C}_{\text{xx}}$  being the covariance of  $\mathbf{F}_{\text{BB}}\mathbf{s}$ . In (5),  $\mathbf{q}_{\text{B}}$  is the quantization noise with the covariance

$$\mathbf{C}_{\mathbf{q}_{\text{B}}\mathbf{q}_{\text{B}}} = \mathbf{C}_{\mathbf{x}_{\text{q}}\mathbf{x}_{\text{q}}} - \mathbf{A}_{\text{B}}\mathbf{C}_{\text{xx}}\mathbf{A}_{\text{B}}, \quad (7)$$

where  $\mathbf{C}_{\mathbf{x}_{\text{q}}\mathbf{x}_{\text{q}}}$  is obtained through arcsin law [11, eq. (14)]. Note that (7) does not ignore any correlation in  $\mathbf{q}_{\text{B}}$ , and hence achieves a superior performance as compared to (4).

### IV. HYBRID BEAMFORMING FOR ONE-BIT DACS

In order to derive the desired precoders  $\mathbf{F}_{\text{RF}}$  and  $\mathbf{F}_{\text{BB}}$ , we first incorporate the linear models (2) and (5) into the observation model (1), which can be jointly represented as

$$\mathbf{y} = \mathbf{H}_{\text{e}}\mathbf{F}_{\text{BB}}\mathbf{s} + \tilde{\mathbf{n}}, \quad (8)$$

where  $\mathbf{H}_{\text{e}} = \mathbf{H}\mathbf{F}_{\text{RF}}\mathbf{A}_{\text{c}}$  is the effective channel seen by the baseband precoder, and  $\tilde{\mathbf{n}} = \mathbf{H}\mathbf{F}_{\text{RF}}\mathbf{q}_{\text{c}} + \mathbf{n}$  is the aggregate noise composed of observation noise and scaled quantization noise, with the subscript  $c \in \{\text{Q}, \text{B}\}$ . In the rest of the paper, we drop the subscript of  $\mathbf{A}_{\text{c}}$  and  $\mathbf{C}_{\mathbf{q}_{\text{c}}\mathbf{q}_{\text{c}}}$  whenever the expressions are common to AQNM and the Bussgang schemes.

Although  $\tilde{\mathbf{n}}$  is not necessarily Gaussian, a lower bound on the achievable rate—considering the fact that the mutual information is the worst for Gaussian noise [12]—is given as

$$R_{\text{ach}} = \log_2 \left| \mathbf{I}_{N_r} + \frac{P_s}{N_s} \mathbf{C}_{\tilde{\mathbf{n}}\tilde{\mathbf{n}}}^{-1} \mathbf{H}_{\text{e}}\mathbf{F}_{\text{BB}}\mathbf{F}_{\text{BB}}^H \mathbf{H}_{\text{e}}^H \right|, \quad (9)$$

where  $\mathbf{C}_{\tilde{\mathbf{n}}\tilde{\mathbf{n}}}$  is the covariance of  $\tilde{\mathbf{n}}$  given by

$$\mathbf{C}_{\tilde{\mathbf{n}}\tilde{\mathbf{n}}} = \mathbf{H}\mathbf{F}_{\text{RF}}\mathbf{C}_{\mathbf{q}_{\text{c}}\mathbf{q}_{\text{c}}}\mathbf{F}_{\text{RF}}^H \mathbf{H}^H + \sigma_n^2 \mathbf{I}_{N_r}. \quad (10)$$

The optimization problem to obtain  $\mathbf{F}_{\text{RF}}$  and  $\mathbf{F}_{\text{BB}}$  can then be formulated to maximize the achievable rate in (9) as follows

$$\max_{\mathbf{F}_{\text{RF}}, \mathbf{F}_{\text{BB}}} R_{\text{ach}}, \quad (11)$$

$$\text{s.t. } \|\mathbf{F}_{\text{RF}}\mathcal{Q}(\mathbf{F}_{\text{BB}}\mathbf{s})\|_{\text{F}}^2 \leq P_{\text{max}}, \quad (11a)$$

$$|[\mathbf{F}_{\text{RF}}]_{m,n}| = \frac{1}{\sqrt{N_t}}, \forall m, n, \quad (11b)$$

where (11a) is the power constraint taking into account (1) and the maximum transmit signal power  $P_{\text{max}}$ , and (11b) is due to the assumption that the RF precoder is composed of finite-quantized phase shifters. Incorporating (2) and (5), and the fact that data and quantization noise is independent of the transmitted data, the power of the transmitted data becomes

$$\|\mathbf{F}_{\text{RF}}\mathcal{Q}(\mathbf{F}_{\text{BB}}\mathbf{s})\|_{\text{F}}^2 = \frac{P_s}{N_s} \|\mathbf{F}_{\text{RF}}\mathbf{A}_{\text{B}}\mathbf{F}_{\text{BB}}\|_{\text{F}}^2 + \text{tr}(\mathbf{F}_{\text{RF}}\mathbf{C}_{\mathbf{q}_{\text{Q}}\mathbf{q}_{\text{Q}}}\mathbf{F}_{\text{RF}}^H), \quad (12)$$

$$= \frac{P_s}{N_s} \|\mathbf{A}_{\text{B}}\mathbf{F}_{\text{BB}}\|_{\text{F}}^2 + \text{tr}(\mathbf{C}_{\mathbf{q}_{\text{Q}}\mathbf{q}_{\text{Q}}}), \quad (13)$$

which follows from the assumption of semi-unitary  $\mathbf{F}_{\text{RF}}$  [4].

### V. ITERATIVE PRECODER DESIGN

We adopt alternating-optimization strategy to optimize  $\mathbf{F}_{\text{RF}}$  and  $\mathbf{F}_{\text{BB}}$  separately, rather than solving (11) for these two precoders jointly which is computationally far too expensive.

#### A. RF Precoder Design

We compute the initial  $\mathbf{F}_{\text{RF}}$  using SVD of the channel matrix, i.e.,  $\mathbf{H} = \mathbf{U}\Sigma\mathbf{V}^H$ . In particular, we form the candidate RF precoder  $\hat{\mathbf{F}}_{\text{RF}}$  by using  $N_{\text{RF}}$  columns of  $\mathbf{V}$  which correspond to the largest  $N_{\text{RF}}$  singular values of  $\mathbf{H}$  (i.e., diagonals of  $\Sigma$ ). Although columns of  $\mathbf{V}$  satisfy constant-norm constraint in (11b), we employ the well-known alternating projection algorithm (APA) to meet semi-unitary constraint [4], as well. This algorithm iteratively projects the RF precoder onto the vector space composed of constant-norm matrices, and projects it back to the semi-unitary matrix space until a convergence criterion is met.

The SVD-based RF precoder design is suitable for the initial iteration of the alternating-optimization precoder design where the baseband precoder  $\mathbf{F}_{\text{BB}}$ , covariance of the quantization distortion  $\mathbf{C}_{\mathbf{q}_{\text{B}}\mathbf{q}_{\text{B}}}$ , and weight matrix  $\mathbf{A}_{\text{B}}$  are all yet to be computed. Once  $\mathbf{F}_{\text{BB}}$  is obtained in the baseband precoder design phase,  $\mathbf{C}_{\mathbf{q}_{\text{B}}\mathbf{q}_{\text{B}}}$  and  $\mathbf{A}_{\text{B}}$  can be computed by (6) and (7), respectively. Then, we propose a new RF precoder that is redesigned so as to maximize the achievable rate directly (instead of relying on SVD of the channel as in the initial iteration) as follows

$$\max_{\varphi_{mn} \in \mathcal{S}_{\varphi} \forall m, n} R_{\text{ach}}, \quad (14)$$

$$\text{s.t. } \frac{P_s}{N_s} \|\mathbf{A}_{\text{B}}\mathbf{F}_{\text{BB}}\|_{\text{F}}^2 + \text{tr}(\mathbf{C}_{\mathbf{q}_{\text{B}}\mathbf{q}_{\text{B}}}) \leq P_{\text{max}}, \quad (14a)$$

where  $\varphi_{mn}$  is the finite-quantized phase of the  $(m, n)$ th entry of the RF precoder (i.e.,  $[\mathbf{F}_{\text{RF}}]_{m,n} = \frac{1}{N_t} e^{j\varphi_{mn}}$ ), and  $\mathcal{S}_{\varphi} = \{-\pi, -\pi + \Delta, \dots, \pi\}$  with  $\Delta$  being the resolution of

the phase shifters. Once the candidate RF precoder is found by (14), we carry out APA to satisfy the semi-unitary condition.

Note that although there are various methods to solve the optimization problem in (14) for the optimal RF precoder, we adopt a greedy based approach seeking for the best phase values for each entry separately [5]. The respective number of searches is  $\lceil \frac{2\pi}{\Delta} \rceil \times N_t \times N_{\text{RF}}$ , which is not prohibitive for moderate array size and  $\Delta$ . Note also that we employ the weight matrix  $\mathbf{A}_B$  and the covariance  $\mathbf{C}_{q_B q_B}$ , which are both based on the Busgang theorem, in (14) after the initial iteration of the alternating-optimization precoder design. By this way, the proposed design procedure gets rid of the shortcoming of AQNM, which ignores the correlation between entries of the quantization distortion, as discussed in Section III.

### B. Baseband Precoder Design

We adopt an SVD-based strategy to find the optimal baseband precoder  $\mathbf{F}_{\text{BB}}$ . Different from the initial SVD-based RF precoder design, the effective channel seen by the baseband precoder is now represented by  $\mathbf{H}_e$  in (8), which is composed of not only the channel  $\mathbf{H}$  but also the RF precoder  $\mathbf{F}_{\text{RF}}$  and the weight matrix  $\mathbf{A}_c$ , with  $c \in \{Q, B\}$ . We therefore take into account  $\mathbf{H}_e$  while designing the baseband precoder, which is different from [6] where any contribution of  $\mathbf{F}_{\text{RF}}$  and  $\mathbf{A}_c$  are ignored. In particular, we compute  $\mathbf{H}_e = \mathbf{U}_e \Sigma_e \mathbf{V}_e^H$ , and use the first  $N_s$  columns of  $\mathbf{V}_e$  to obtain a candidate baseband precoder  $\hat{\mathbf{F}}_{\text{BB}}$  assuming the diagonals  $\Sigma_e$  are sorted in descending order.

Note that since  $\mathbf{A}_B$  of the Busgang theorem given in (6) is a direct function of  $\mathbf{F}_{\text{BB}}$ , which is yet to be designed for the initial iteration, we employ  $\mathbf{A}_Q$  of AQNM given in (3) while obtaining  $\mathbf{H}_e$  since it is readily available. Once  $\mathbf{F}_{\text{BB}}$  becomes available from the previous iterations, we use  $\mathbf{A}_B$  in  $\mathbf{H}_e$  to seek a better performance. Note also that the final baseband precoder  $\mathbf{F}_{\text{BB}}$  should satisfy the power constraint in (13). We therefore normalize the power of candidate precoder  $\hat{\mathbf{F}}_{\text{BB}}$  as

$$\mathbf{F}_{\text{BB}} = \left[ \frac{P_{\max} - \text{tr}(\mathbf{C}_{q_Q q_Q})}{\frac{P_s}{N_s} \|\mathbf{A}_c \hat{\mathbf{F}}_{\text{BB}}\|_F^2} \right]^{\frac{1}{2}} \hat{\mathbf{F}}_{\text{BB}}, \quad (15)$$

where  $c = Q$  ( $c = B$ ) for the first (subsequent) iteration(s).

As discussed in Section III, the covariance in (7) is superior to (4) as it takes into account the correlation over the quantization distortion. This covariance matrix is, however, a function of not only  $\mathbf{F}_{\text{BB}}$ , for which no estimate is available for the initial iteration, but also  $\mathbf{A}_B$ , which depends on  $\mathbf{F}_{\text{BB}}$  too through (6). In order to facilitate the derivation, we therefore employ the AQNM-based covariance  $\mathbf{C}_{q_Q q_Q}$  given by (4), which is a direct function of  $\mathbf{F}_{\text{BB}}$ , while performing the power normalization in (15) for the initial iteration. Unfortunately, obtaining  $\mathbf{C}_{q_Q q_Q}$  is still cumbersome as it should be computed along with  $\mathbf{F}_{\text{BB}}$  because of the mutual dependency.

In [6], the baseband precoder is derived assuming a sufficiently high-resolution DAC, and, hence, the covariance is simply assumed to be a zero matrix in power constraint computations. In our case, resolution of DAC is 1-bit, and the zero-covariance assumption (i.e.,  $\mathbf{C}_{q_Q q_Q} = \mathbf{0}_{N_{\text{RF}}}$ ), hence, does not hold. We therefore propose a fixed-point iterative solution to find optimal  $\mathbf{F}_{\text{BB}}$  and  $\mathbf{C}_{q_Q q_Q}$  jointly [11]. As described in

Algorithm 1, we start by assuming  $\mathbf{C}_{q_Q q_Q} = \mathbf{0}_{N_{\text{RF}}}$ , and recursively update  $\mathbf{F}_{\text{BB}}$  by (15) and  $\mathbf{C}_{q_Q q_Q}$  by (4) in sequence until a convergence condition (line 6 of Algorithm 1) is achieved for the covariance matrix. In Section VI, we numerically verify a satisfactory convergence behavior for  $\mathbf{C}_{q_Q q_Q}$ .

### Algorithm 1 Alternating-Optimization Algorithm for Hybrid Precoder Design for 1-Bit DAC

- 1: **Initialize:**  $\mathbf{A}_Q$  by (3),  $\mathbf{C}_{q_Q q_Q}^{(\ell)} \leftarrow \mathbf{0}_{N_{\text{RF}}}$ ,  $\ell = -1, 0$ ,  $k \leftarrow 1$ , error tolerance  $\epsilon$ , number of iterations  $K$
- 2: **Initial Iteration:**
- 3: Compute  $\hat{\mathbf{F}}_{\text{RF}}$  by SVD of  $\mathbf{H}$
- 4: Compute  $\mathbf{F}_{\text{RF}}$  by applying APA [4] to  $\hat{\mathbf{F}}_{\text{RF}}$
- 5: Compute  $\hat{\mathbf{F}}_{\text{BB}}$  by SVD of  $\mathbf{H}_e = \mathbf{H} \mathbf{F}_{\text{RF}} \mathbf{A}_Q$
- 6: **while**  $\|\mathbf{C}_{q_Q q_Q}^{(k-1)} - \mathbf{C}_{q_Q q_Q}^{(k-2)}\|_F / N_{\text{RF}} > \epsilon$  **do**
- 7:   Update  $\mathbf{F}_{\text{BB}}$  by (15) using  $\mathbf{C}_{q_Q q_Q}^{(k-1)}$
- 8:   Compute  $\mathbf{C}_{q_Q q_Q}^{(k)}$  by (4)
- 9:    $k \leftarrow k + 1$
- 10: **end while**
- 11: **Subsequent Iterations:**
- 12: **for**  $i = 2, \dots, K$  **do**
- 13:   Update  $\mathbf{A}_B$  and  $\mathbf{C}_{q_B q_B}$  by (6) and (7)
- 14:   Update  $\hat{\mathbf{F}}_{\text{BB}}$  by SVD of  $\mathbf{H}_e = \mathbf{H} \mathbf{F}_{\text{RF}} \mathbf{A}_B$
- 15:   Update  $\mathbf{F}_{\text{BB}}$  by (15) using  $\mathbf{C}_{q_B q_B}$
- 16:   Compute  $\hat{\mathbf{F}}_{\text{RF}}$  by (14)
- 17:   Compute  $\mathbf{F}_{\text{RF}}$  by applying APA [4] to  $\hat{\mathbf{F}}_{\text{RF}}$
- 18: **end for**

## VI. NUMERICAL RESULTS

In this section, we present the numerical results based on extensive Monte Carlo simulations to evaluate the performance of proposed hybrid precoder design assuming one-bit DAC. The simulation parameters are listed in Table I.

TABLE I  
SIMULATION PARAMETERS

Parameter	Value
Number of Tx antennas ( $N_t$ )	32
Number of Rx antennas ( $N_r$ )	8
Number of RF chains ( $N_{\text{RF}}$ )	{4, 8}
Number of streams ( $N_s$ )	$N_{\text{RF}}$
Maximum transmit signal power ( $P_{\max}$ )	10 Watts
Power of the unprecoded data ( $P_s$ )	1 Watt
Number of clusters ( $N_c$ )	1
Number of rays ( $N_p$ )	5
Angular distribution of clusters	Uniform
Angular distribution of rays	Laplace
Angular spread of rays	10°
Resolution of the phase shifters ( $\Delta$ )	5°

In Fig. 2, we depict the convergence behavior of the covariance matrix  $\mathbf{C}_{q_Q q_Q}$  by lines 6–10 of Algorithm 1. We observe that the normalized distance (i.e., line 6 of Algorithm 1) converges (i.e., hits the precision limit of the computer in use) after a finite number of iterations for any choice of  $N_{\text{RF}}$ . We therefore verify that it is possible to obtain a non-zero  $\mathbf{C}_{q_Q q_Q}$  through fixed-point iterations which produces more accurate rates since it does not ignore the quantization distortion.

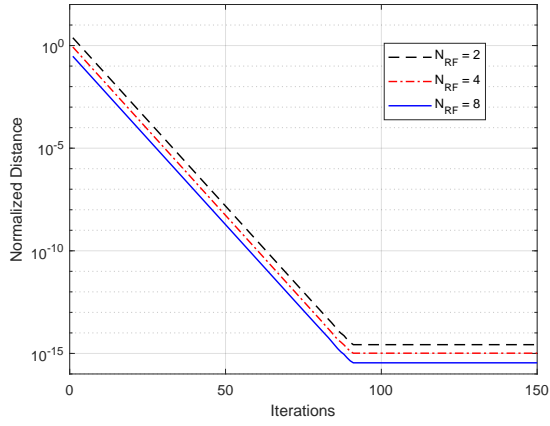
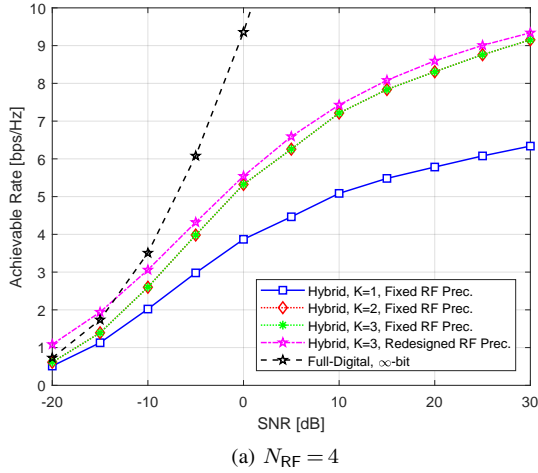
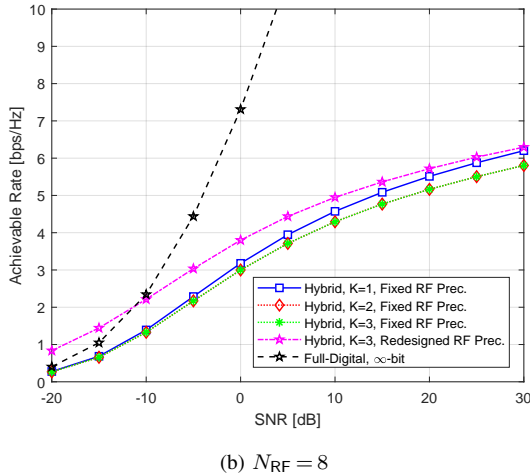


Fig. 2. Convergence of  $\mathbf{C}_{q_0q_0}$  for  $N_{RF} \in \{2, 4, 8\}$ .



(a)  $N_{RF} = 4$



(b)  $N_{RF} = 8$

Fig. 3. The achievable rate against varying SNR for  $N_{RF} \in \{4, 8\}$ , number of iterations  $K \in \{1, 2, 3\}$ , with fixed and redesigned RF precoder.

In Fig. 3, we present the achievable rate results against varying signal-to-noise ratio (SNR), which is defined as  $P_{\max}/\sigma_n^2$ , for  $N_{RF} \in \{4, 8\}$ . For comparison purposes, we also include the performance of the SVD-based full-digital precoder  $\mathbf{F}_{FD}$  with infinite-resolution DACs. Note that the performance is better in  $N_{RF} = 4$  than  $N_{RF} = 8$ , since spatially correlated mmWave channel is not decomposed into full dimensional orthogonal sub-channels in the latter. In Fig. 3(a), which assumes  $N_{RF} = 4$ , the achievable rate improves after the initial iteration of the overall alternating-optimization algorithm, even when  $\mathbf{F}_{RF}$  is kept the same (i.e., without implementing the

lines 16-17 of Algorithm 1). Since the initial iteration employs the AQNM-based weight and covariance matrices, this performance improvement is basically due to the use of  $\mathbf{A}_B$  and  $\mathbf{C}_{q_Bq_B}$ , which are both based on the Bussgang theorem (i.e., line 13 of Algorithm 1). We would like to remind that performance of even the initial iteration is associated with the recursive computation of the covariance  $\mathbf{C}_{q_0q_0}$  instead of assuming it is simply a zero matrix.

We also observe that redesigning  $\mathbf{F}_{RF}$  (i.e., lines 16-17 of Algorithm 1) improves the performance even further. Since  $\mathbf{F}_{RF}$  redesign aims at directly maximizing the achievable rate by (14), the respective performance is superior to that of the full-digital precoder at low SNR, which solely relies on SVD of the channel. We observe a similar behavior in Fig. 3(b) for  $N_{RF} = 8$ . Since the number of multiplexed streams now doubles, the subsequent iterations of the alternating-optimization algorithm without  $\mathbf{F}_{RF}$  redesign cannot help improve the achievable rate, and even worsen it at high SNR. Despite that,  $\mathbf{F}_{RF}$  redesign achieves even a larger performance gap than  $N_{RF} = 4$  in this challenging environment as compared to the fixed  $\mathbf{F}_{RF}$  case.

## VII. CONCLUSION

We propose a hybrid precoder for spatially correlated mmWave channels equipped with one-bit DAC and finite-quantized phase shifters. We carefully incorporate the impact of the quantization distortion, and obtain the baseband and RF precoders relying on the Bussgang theorem. The numerical results verify the superiority of the proposed alternating-maximization algorithm as compared to AQNM-based design.

## REFERENCES

- [1] T. S. Rappaport *et al.*, "Overview of millimeter wave communications for fifth-generation (5G) wireless networks—with a focus on propagation models," *IEEE Trans. Antennas Propag.*, vol. 65, no. 12, pp. 6213–6230, Dec. 2017.
- [2] O. E. Ayach *et al.*, "Spatially sparse precoding in millimeter wave MIMO systems," *IEEE Trans. Wireless Commun.*, vol. 13, no. 3, pp. 1499–1513, Mar. 2014.
- [3] A. K. Saxena, I. Fijalkow, and A. L. Swindlehurst, "Analysis of one-bit quantized precoding for the multiuser massive MIMO downlink," *IEEE Trans. Signal Process.*, vol. 65, no. 17, pp. 4624–4634, Sep. 2017.
- [4] J. Mo *et al.*, "Hybrid architectures with few-bit ADC receivers: Achievable rates and energy-rate tradeoffs," *IEEE Trans. Wireless Commun.*, vol. 16, no. 4, pp. 2274–2287, 2017.
- [5] Q. Hou *et al.*, "Hybrid precoding design for MIMO system with one-bit ADC receivers," *IEEE Access*, vol. 6, pp. 48 478–48 488, 2018.
- [6] L. N. Ribeiro *et al.*, "Energy efficiency of mmWave massive MIMO precoding with low-resolution DACs," *IEEE J. Sel. Topics Signal Process.*, vol. 12, no. 2, pp. 298–312, 2018.
- [7] J. J. Bussgang, "Crosscorrelation functions of amplitude-distorted gaussian signals," *MIT Res. Lab. Electron.*, May 1952, Tech. Rep. 216.
- [8] O. Orhan, E. Erkip, and S. Rangan, "Low power analog-to-digital conversion in millimeter wave systems: Impact of resolution and bandwidth on performance," in *Proc. IEEE ITA*, Feb. 2015, pp. 191–198.
- [9] B. Li, N. Liang, and W. Zhang, "On transmission model for massive MIMO under low-resolution output quantization," in *Proc. IEEE Vehic. Technol. Conf. (VTC2017-Spring)*, Jun. 2017, pp. 1–5.
- [10] J. Max, "Quantizing for minimum distortion," *IRE Trans. Inf. Theory*, vol. 6, no. 1, pp. 7–12, Mar. 1960.
- [11] Y. Yaprıcı *et al.*, "SLNR based precoding for one-bit quantized massive MIMO in mmWave communications," in *Proc. IEEE Int. Conf. Commun. (ICC) Workshops*, Shanghai, China, May 2019.
- [12] A. Mezghani and J. A. Nossek, "Capacity lower bound of MIMO channels with output quantization and correlated noise," in *Proc. IEEE Int. Symp. Inf. Theory (ISIT)*, Jul. 2012.